RSC Advances

ROYAL SOCIETY OF CHEMISTRY

www.rsc.org/advances

Cite this: DOI: 10.1039/c0xx00000x

www.rsc.org/xxxxxx

ARTICLE TYPE

A novel tunable $Na_2Ba_6(Si_2O_7)(SiO_4)_2$:$Ce^{3+}$,$Mn^{2+}$ phosphor with excellent thermal stability for white light emitting diodes

Wenzhen Lv,[a, b] Yongchao Jia,[a, b] Qi Zhao,[a, b] Mengmeng Jiao,[a, b] Baiqi Shao,[a, b] Wei Lv,[a] and Hongpeng You *[a]

Received (in XXX, XXX) Xth XXXXXXXXX 20XX, Accepted Xth XXXXXXXXX 20XX
DOI: 10.1039/b000000x

In this paper, Ce^{3+} doped and Ce^{3+},Mn^{2+} co-doped $Na_2Ba_6(Si_2O_7)(SiO_4)_2$ phosphor were synthesized via high temperature solid-state reaction. The Rietveld refinement analysis of the x-ray diffraction patterns confirmed the formation of the single phase of $Na_2Ba_6(Si_2O_7)(SiO_4)_2$. The PL spectrum of the Ce^{3+} single-doped phosphor shows a broad asymmetric band extending from 350 to 600 nm peaking at 420 nm under the excitation of UV light. Also, the low temperature (5 K) PL spectrum shows clearly three peaks at 375 nm, 420 nm and 451nm, which is in accord with the Ce^{3+} ions site in the host. The Ce^{3+},Mn^{2+} co-doped phosphors show a blue emission band and an orange emission band, and the corresponding CIE coordinates intuitively indicate the tunable colors from the blue to green area. And the involved the energy transfer mechanism from Ce^{3+} to Mn^{2+} in the host has been verified to be a dipole-quadrupole interaction. In addition, the emission intensity of $Na_2Ba_6(Si_2O_7)(SiO_4)_2$:0.01$Ce^{3+}$ phosphor slightly changed with the temperature increase from 300 to 450K, revealing that the obtained phosphor possesses an excellent thermal stability, which makes it an attractive candidate phosphor for white lighting emitting diodes.

1. Introduction

In the past decade, solid-state white lighting emitting has confirmed its irreplaceable status as new solid-state light sources in the context of environmental and energy saving issues. As a result, phosphors, as an important part of white lighting emitting have aroused worldwide research interest. [1-3] Phosphors, as an important part of WLEDs has aroused worldwide research interest. Phosphors are always composed of the two indispensable compositions as the matrix and luminescence center. Talking about phosphors, we have to mention the two indispensable compositions as the matrix and luminescence center. The matrix is always developed from the various compounds. Always, silicate with diverse, rigid and very stable structures have been investigated widely for either their physicochemical phenomena and mechanisms or available application and practical usage in phosphor.[4]Among various silicate compounds, Sr_3SiO_5 has been highlighted and chosen as an matrix for many years, because the Sr_2SiO_5 doped with Ce^{3+} ion phosphor shows excellent performance as a yellow component for WLEDs.[5-6] As to the luminescence center, we have to mention Ce^{3+} ion, which always acted as the luminesce centers in phosphor. The Ce^{3+} ion can be excited by either a UV chip or a blue chip. The emission band of Ce^{3+} ion is usually composed of a broad band and varies from ultraviolet to yellow, depending on the host, which is caused by the Ce^{3+} ion $4f^1$ ground state undergoing parity allowed f–d transition with 5d as the excited state on excitation. [7] Therefore, matrices doped with Ce^{3+} ions show great potential as phosphor for white lighting emitting diodes, and indeed receive a lot of attention recently. As a result, many useful phosphors have been reported successively.[8-9]The famous Ce^{3+} doped yellow phosphor is $Y_3Al_5O_{12}$:Ce^{3+}, however, the phosphor suffers a low R_a when pumped by a blue LED chip, which is caused by the lack of thermal stability at elevated temperatures during white LED operation. Therefore, most researchers are committed on developing novel phosphors with improved thermal stability now. In addition, the Ce^{3+} ion, apart from its own intense emission, can facilitate the energy transfer to various luminescent centers such as Tb^{3+} ion or Mn^{2+} ion, which can significantly solve the overheating problem associated with inappropriate excitation for WLEDs. [10-11]

Here, we choose $Na_2Ba_6(Si_2O_7)(SiO_4)_2$ matrix as a research objectives.Notwithstanding the fact that the $Na_2Ba_6(Si_2O_7)(SiO_4)_2$ matrix has been first reported by Tamazyan et al, [12] the most interesting feature of the co-existence structure of Si_2O_7 and SiO_4 in the $Na_2Ba_6(Si_2O_7)(SiO_4)_2$ matrix has not attracted much attention from materials scientists until recently. Also, to our best knowledge, neither investigations regarding on the luminescence properties of $Na_2Ba_6(Si_2O_7)(SiO_4)_2$ nor the energy transfer mechanism from Ce^{3+} to Mn^{2+} in the host has been reported. Therefore, we speculate whether the unique structure doped with Ce^{3+} or Mn^{2+} can produce some surprising phenomenon. Here,

[a] *State Key Laboratory of Rare Earth Resource Utilization, Changchun Institute of Applied Chemistry, Chinese Academy of Sciences, Changchun, 130022, P. R. China. E-mail: hpyou@ciac.ac.cn*

[b] *Graduate School of the Chinese Academy of Sciences, Beijing, 100049, P. R. China*

we focus on investigating the crystal structure, the thermal stability and the luminescent properties of Ce^{3+} or Ce^{3+},Mn^{2+} doped $Na_2Ba_6(Si_2O_7)(SiO_4)_2$ phosphors. The result indicates that this novel developed phosphor has excellent thermal stability and shows tunable blue to yellow emission excited by UV light.

2. Experimental section

2.1 Materials Synthesis.

Polycrystalline powder samples with the compositions of $Na_2Ba_6(Si_2O_7)(SiO_4)_2$: xCe^{3+}, yMn^{2+} (NBSO:Ce^{3+},Mn^{2+})were synthesized via a conventional solid-state reaction with $NaNO_3$ (A.C), $BaCO_3$ (A.C), SiO_2(A.C),CeO_2 (99.99%) and $MnCO_3$(99.99%) as the raw materials. The stoichiometric amounts of the raw materials were weighed out and thoroughly mixed by grinding in an agate mortar. Afterward, the obtained product was then annealed at 1050 °C for 8 h with an intermediate regrinding under a 5% H_2 - 95% N_2 atmosphere. Finally, the temperature lowered to room temperature and some white polycrystalline powder was obtained.

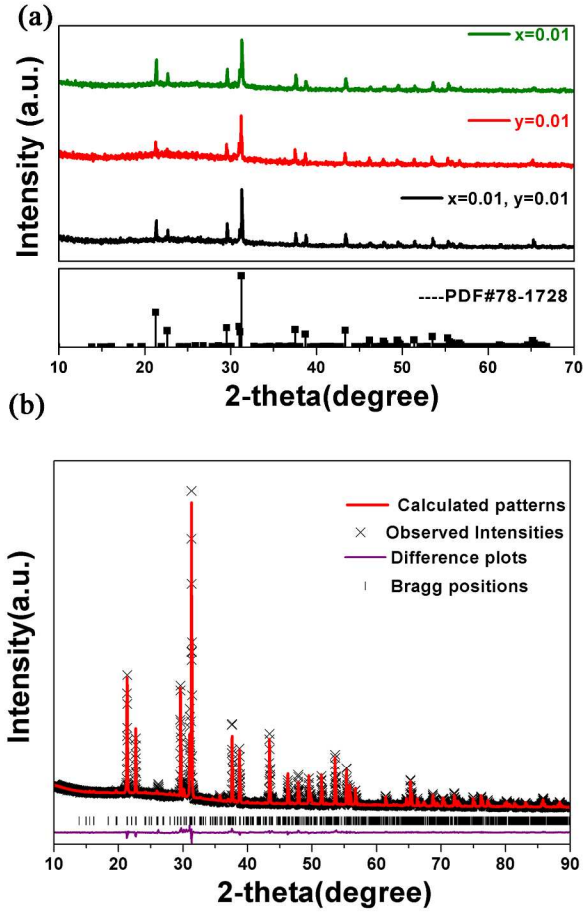

Fig.1 Results of structure refinement of x-ray diffraction patterns for $Na_2Ba_6(Si_2O_7)(SiO_4)_2$: 0.01Ce

1.1 Characterization.

The crystalline phases of the samples were identified by x-ray diffraction (XRD), which were performed on a D8 Focus diffractometer (Bruker) operating at 40 kV and 40 mA with Cu *K*α radiation. The X-ray diffraction data were recorded as follows: 2θ range: 15°-70°, scanning speed: 0.5min, 0.02step. The powder diffraction datawere subjected to performa computer software General Structure Analysis System (GSAS) package.[13]The photoluminescence (PL) and photoluminescence excitation (PLE) spectra of the obtained powders were recorded with a Hitachi F-4500 spectrophotometer equipped with a 150 W xenon lamp as the excitation source. Thermoluminescence (TL) spectra were measured with a three-dimensional (3D)- TSL spectra instrument. The luminescence decay curve was obtained from a Lecroy Wave Runner 6100 digital oscilloscope (1GHz) using a tunable laser (pulse width = 4 ns, gate = 50 ns) as the excitation source (Continuum Sunlite OPO). All the measurements were performed at room temperature.

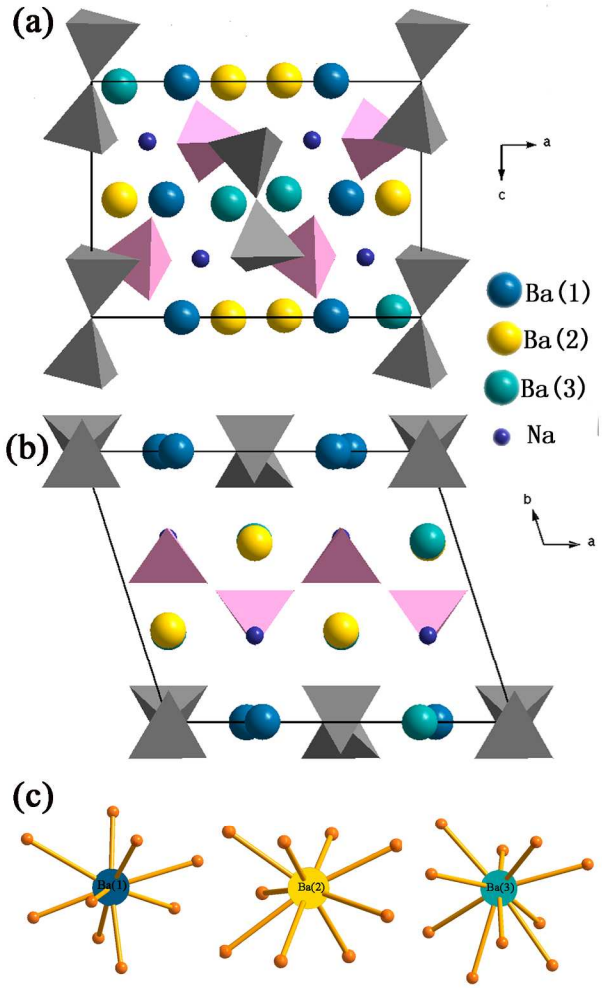

Fig. 2 Crystal structure of $Na_2Ba_6(Si_2O_7)(SiO_4)_2$ in different directions **(a)** and **(b);** Coordination of three different Ba^{2+} ions**(c).**

2. Results and discussion

3.1 $Na_2Ba_6(Si_2O_7)(SiO_4)_2$:$Ce^{3+}$ Phosphor

Fig. 1(a) shows the x-ray diffraction patterns of several representive $Na_2Ba_6(Si_2O_7)(SiO_4)_2$:0.01$Ce^{3+}$,$yMn^{2+}$ samples. It is obvious that all the diffraction peaks of the samples can be exactly indexed to the standard data of $Na_2Ba_6(Si_2O_7)(SiO_4)_2$ (JCPDS card no.78-1728)， which indicates that the prepared phosphors are of single phase and the doped Ce^{3+} and Mn^{2+} ions have been incorporated into the host successfully. To further

investigate the structure of of the $Na_2Ba_6(Si_2O_7)(SiO_4)_2$ host, Revield refinement of the x-ray diffraction patterns of the $Na_2Ba_6(Si_2O_7)(SiO_4)_2$:0.01$Ce^{3+}$ sample has been done at room temperature **as Fig. 1(b)** shows.[13] The initial structural model was constructed with crystallographic data previously reported for $Na_2Ba_6(Si_2O_7)(SiO_4)_2$ (JCPDS78-1728). The crystallographic cell parameters proceeded smoothly to convergence and do not show significant change considering the standard deviations. All of the observed peaks satisfy the reflection condition, χ^2 = 7.85, R_p = 6.28% and R_{wp} = 8.819%. The refinement result indicates the $Na_2Ba_6(Si_2O_7)(SiO_4)_2$ has space group $P2_1/a$ with unit cell parameters a =11.52 Å, b =9.508 Å, c = 7.856 Å, V= 820.64Å^3, and Z = 2. Meanwhile, the refinement result further verifies that the structure of $Na_2Ba_6(Si_2O_7)(SiO_4)_2$ host is unchanged with the doping of luminescence ions.

Fig. 2 **(a)** and **(b)** represents a spatial view of the $Na_2Ba_6(Si_2O_7)(SiO_4)_2$ unit cell from different directions. One can see clearly the discrete [SiO_4] anions (pink polohedron)and isolated [Si_2O_7] anions(gray polohedron) in this unit cell. The discrete [SiO_4] anions and isolated [Si_2O_7] anions form unique layer in sandwich package way. The isolated [SiO_4] anions arrange in the inside of the cell, while the isolated [Si_2O_7] anions occupy the upper and lower plane. The entire above package manner to delimit right coordination cavities occupied by Ba^{2+} and Na^+ cations, respectively. There are three crystallographic independent Ba^{2+} ions positions denoted as Ba(1), Ba(2), and Ba(3), in which Ba(1) and Ba(2) are in 9-coordination environment with tricapped trigonal prismatic geometry, while Ba(3) occupies 10-coordinated O polyhedra constructing bicapped square prism which builds distorted polyhedron with oxygens interconnected via common edges, respectively. **Fig. 2(c)** displays the different coordination environments of the three Ba^{2+} ions. Another cation in the host, the Na^+ ion is all coordinated by six oxygen atoms in the form of an octahedra. On the basis of the above structure analysis, the coordination diversity of the Ba^{2+} sites in the host is benefit to the luminescence. [12]

Fig. 3(a) shows the PLE and PL spectra of $Na_2Ba_6(Si_2O_7)(SiO_4)_2$:0.01$Ce^{3+}$. The PLE spectrum is composed of a broad band range from 200 to 400 nm, a characteristic feature of the Ce^{3+} ions emission band from the $4f^1$ ground state to the 5*d* level as described by Judd–Ofelt theory.The PL spectrum shows a broad asymmetric band extending from 350 to 600 nm peaking at 420 nm.[14,15] The asymmetry of PL band is always caused by the various luminescence sites in the host. Always, the value of Stokes Shift is an imporant property of PL spectrum, which can measure the stiff of host lattice and the degree of the nonradiative relaxation after the luminescent ions excited. The Stokes Shift can be roughly estimated as twice of the energy difference between the peak energy of the emission band and the zero-phonon line energy that was empirically determined as the intersection point of the excitation spectrum and emission spectrum. [16] The Stokes Shift of emission is roughly calculated to be 0.694 eV in energy here. In order to better understand the photoluminescence property of Ce^{3+} ion, we measure the PL spectrum of $Na_2Ba_6(Si_2O_7)(SiO_4)_2$:0.01$Ce^{3+}$ at 5 K (**Fig. 3(b)**). The emission curve has been well-fitted with a sum of three Gaussian functions in energy. One can see clearly a broad band with three peaks at 375, 420 and 451 nm, respectively. These components can be ascribed to the contributions of the transitions from the lowest 5d excited states to the ground states in three different Ce^{3+} luminescence centres, which is in accord with the number of Ba^{2+} sites in the host. It has been suggested the d-band edge (E) in energy of Ce^{3+} ion emission is sensitive to electron–electron repulsion, which always obey an empirical relation by Van Uitert as following:[17]

$$E(cm^{-1}) = Q^*\left[1-\left(\frac{V}{4}\right)^{\frac{1}{V}}\right]\times 10^{\frac{-(nEar)}{80}}$$

Here Q^* is the position in energy for the lower d-band edge for

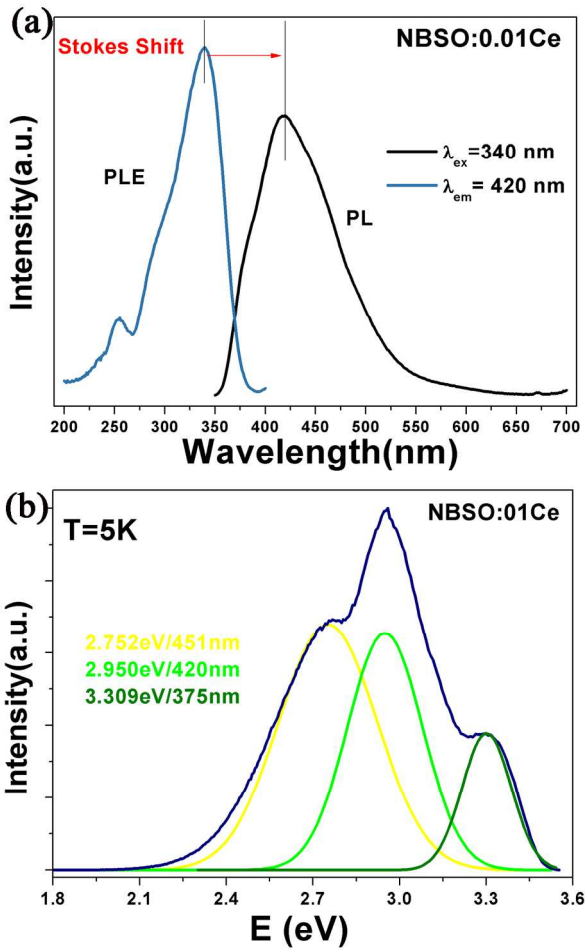

Fig. 3 PLE spectrum observed at 420nm **(a);** PL spectrum of $Na_2Ba_6(Si_2O_7)(SiO_4)_2$:0.01$Ce^{3+}$ at room temperature and 5K under excited at 330nm **(b).**

the free Ce^{3+} ion (Q^*= 50000 cm^{-1}), E is the position for the Ce^{3+} ion emission peak, V is the valence of the Ce^{3+} ion (V = 3), n is the number of anions in the immediate shell about the Ce^{3+}ion, Ea is the electron affinity of the atoms (eV), and r is the radius of the host cation replaced by Ce^{3+} ion (Å). Ea is a constant in the same host. Here, V = 3, Q^*= 50000 cm^{-1}, the value of E is directly proportional to the product of n and r. In our case, Ba(1) and Ba(2) sites are nine-coordinated by nine O atoms with Ba-O distance of 2.890 Å and 2.894 Å, respectively. The Ba(3) site is ten-coordinated with O atoms at an average Ba-O distance of 2.938 Å.

Therefore, we can get a conclusion that the band centred at 375 nm is attributed to the 5d - 4f emission of Ce^{3+} ion occupied the Ba(3)ion site with ten-coordinate, and the bands at 451 and 420 nm are due to the Ce^{3+} ion occupied Ba(1) and Ba(2)ion site with nine coordination.

The thermal quenching property is another important technological parameter for phosphors used in practical solid-state lighting. **Fig. 6** indicates the temperature-dependent relative emission intensities of the as-prepared $Na_2Ba_6(Si_2O_7)(SiO_4)_2$:0.01$Ce^{3+}$ phosphor under the 340 nm excitation. With the temperature increasing from room temperature to 450 k, the integrated emission intensity of $Na_2Ba_6(Si_2O_7)(SiO_4)_2$:0.01$Ce^{3+}$ phosphor changes from 100% (300 K) to 93.7% (450 K), indicating that the phosphor possesses a excellent thermal stability. To verify the origin of temperature dependent emission intensity I_T, the activation energy ΔE (the electrons excited from 4f states to the lowest 5d states of Ce^{3+} ion) can be described as the following equation: [18,19]

$$n(\frac{I_0}{I}-1)=\ln C-\frac{\Delta E}{kT}$$

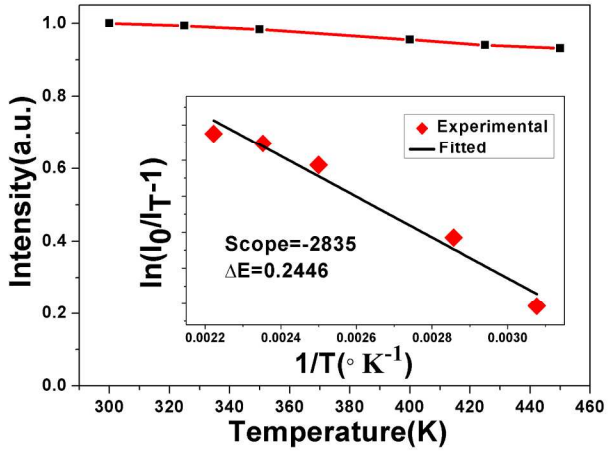

Fig. 4. PL intensity of $Na_2Ba_6(Si_2O_7)(SiO_4)_2$:0.01$Ce^{3+}$ from room temperature to 450K(λ_{ex}= 340 nm). The inset shows the plot ln[(I_0/I_T) - 1] versus 1/ *k* T.

where I_0 and I_T represent the PL intensity of room temperature and testing temperature, respectively; *k* represents Boltzmann constant. The ΔE values for $Na_2Ba_6(Si_2O_7)(SiO_4)_2$:0.01$Ce^{3+}$ were calculateded to be 0.2446 eV as shown inset of **Fig.4.** The larger ΔE ($Na_xCa_{1-x}Al_{2-x}Si_{2+x}O8:Eu^{2+}$ (x = 0.34), ΔE = 0.033 eV; $NaBaScSi_2O_7$, ΔE = 0.081 eV) is can be a theory evidence certisfying the excellent thermal stability of this novel phosphor. [20,21]The excellent thermal stability of the $Na_2Ba_6(Si_2O_7)(SiO_4)_2$:Ce phosphor has aroused our great interest. The unusual features may originate from the bigger Ba^{2+} ions site and the unique crystal chemistry structure. Since the ionic radii of Ce^{3+} ions(CN = 9, R =1.196; CN = 10, R=1.25) is smaller than Ba^{2+} ions(CN = 9, R = 1.47; CN = 10, R = 1.52) with the same coordination in $Na_2Ba_6(Si_2O_7)(SiO_4)$ host lattice. With the increasing temperature, the interaction between the electrons is reduced, so that they spread out over wider orbitals which would result in the increasing covalence of Ce-O, as a result, the surrounding of the activator Ce^{3+} ions will be forced to expand, fortunately, the larger Ba^{2+} ion site makes Ce^{3+} ion match with the surrounding. On the other hand, , another influence factor for the excellent thermal stability can be got from the $Na_2Ba_6(Si_2O_7)(SiO_4)_2$ structure. Compared with other silicate compounds as $Na_xCa_{1-x}Al_{2-x}Si_{2+x}O_8:Eu^{2+}$ (x = 0.34) or $NaBaScSi_2O_7$, the crystal structure here, is composed by discrete [SiO_4] anions and isolated [Si_2O_7] anions, and these anions bulid in a unique stacking mode. The isolated [Si_2O_7] anions construct the main skeleton of $Na_2Ba_6(Si_2O_7)(SiO_4)_2$ host and the discrete [SiO_4] anions inserts into the inner space as **Fig 2(a) and Fig 2(b)** shows. Thus, we speculate that the coexistance of the two different anions and the unique stacking mode in geometry may improve the stability of compounds.[22]

3.2 $Na_2Ba_6(Si_2O_7)(SiO_4)_2$:$Ce^{3+}$,$Mn^{2+}$ Phosphor

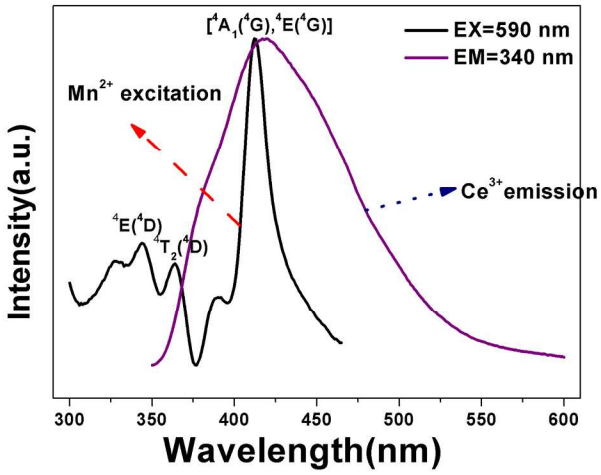

Fig.5 Overlap of Ce^{3+} emission spectrum to the Mn^{2+} excitation spectrum.

As shown in **Fig. 5,** the PL spectrum of $Na_2Ba_6(Si_2O_7)(SiO_4)_2$:0.01$Ce^{3+}$ shows a broadband emission from 350 to 600 nm centered at 420 nm, which was attributed to the f-d transition. The PLE spectrum of $Na_2Ba_6(Si_2O_7)(SiO_4)_2$:0.03$Mn^{2+}$contains several bands centered at 344, 365, and 413 nm, corresponding to the transitions from the $^6A_1(^6S)$ ground state to the $^4E(^4D)$, $^4T_2(^4D)$, and [$^4A_1(4G)$,$^4E(^4G)$] excited states, respectively. The significant spectral overlap between the PL spectrum of $Ce^{3+}$and PLE spectrum of Mn^{2+} indicates that the energy level of Ce^{3+} ions matches with well the energy level of Mn^{2+} ions. Thus, we can expect an effective resonance-type energy transfer from the Ce^{3+} to Mn^{2+} ions. Moreover, as shown in **Fig. 6,** another possible evidence, the PLE spectrum monitoring the emission(585 nm) of the Mn^{2+} and that (420 nm) of Ce^{3+} are similar. Under 340 nm excitation, the PL spectrum of the codoped sample $Na_2Ba_6(Si_2O_7)(SiO_4)_2$: 0.01$Ce^{3+}$,0.01$Mn^{2+}$ in **Fig. 6** shows both a blue band coresponding to the f－d transition of Ce^{3+} ions and a yellow band attributing to the $^4T_1$ － $^6A_1$ transition of Mn^{2+} ions. As a result, we can get various color tunes via adgusting the Mn^{2+} ions content.[23]

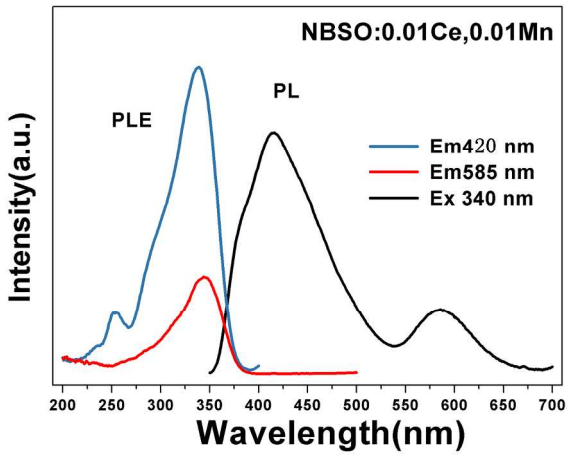

Fig.6 The PLE andPL spectra of $Na_2Ba_6(Si_2O_7)(SiO_4)_2$:0.01$Ce^{3+}$,0.01$Mn^{2+}$.

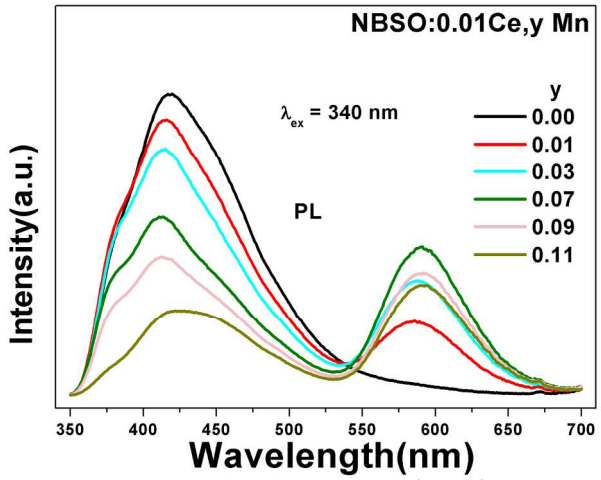

Fig. 7 PL spectra of $Na_2Ba_6(Si_2O_7)(SiO_4)_2$: 0.01$Ce^{3+}$,yMn^{2+} (y = 0.01, 0.03, 0.07, 0.09, 0.11) phosphors under 340nm excitation.

Fig. 7 decipts the PL spectra of several $Na_2Ba_6(Si_2O_7)(SiO_4)_2$: 0.01$Ce^{3+}$,yMn^{2+} (y = 0.01, 0.03, 0.07, 0.09, 0.11) phosphors. We can observe clearly that the PL luminescent intensity of Ce^{3+} ions decreases with the Mn^{2+} ions concentration up to 0.11. However, the emission intensity of Mn^{2+} ions shows an enhancement initially until 0.07, beyond which its intensity shows a drastic reduction.The phonmenons indeed indicate efficient energy transfer from Ce^{3+} to Mn^{2+} ions.

The energy transfer efficiency (η_T) from Ce^{3+} to Mn^{2+}ions in $Na_2Ba_6(Si_2O_7)(SiO_4)_2$: 0.01$Ce^{3+}$,y$Mn^{2+}$ can be calculated by the formula:[24]

$$\eta = 1 - \frac{I_s}{I_{so}}$$

where I_{so} is the intensity of the Ce^{3+} ions and I_s is the intensity of the Ce^{3+} ions in the presence of the Mn^{2+} ions. Thus, the The energy transfer efficiency was calculated and presented in **Fig. 8.** The energy transfer efficiency was found to increase gradually with the increase of the Mn^{2+}concentration. As a result, a rough estimation of the critical distance (R_{sa}) for energy transfer from Ce^{3+} to Mn^{2+} ions can be calculated from the following relationship given by Blasse:

$$R_{sa} = 2R = 2(\frac{3V}{4\pi x_c N})^{1/3}$$

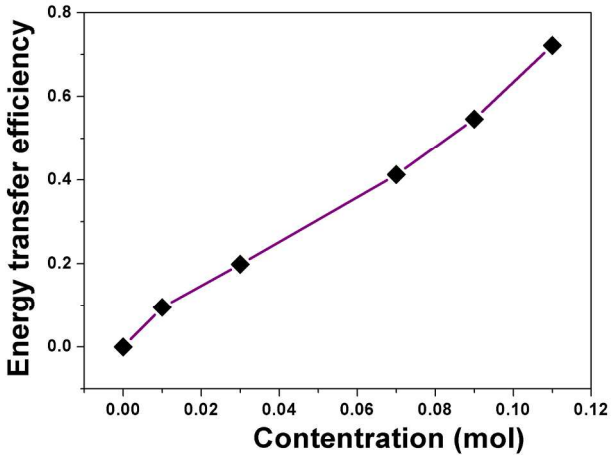

Fig. 8 Energy transfer efficiency from Ce^{3+} to Mn^{2+}.

where V is the volume of the unit cell, x_c is the critical concentration of the activator ion, and N represents the number of sites that the Ce^{3+} ion can occupy in per unit cell. For the $Na_2Ba_6(Si_2O_7)(SiO_4)_2$ host, N =12, x_c = 0.07, and V = 820.64Å^3, Therefore, the R_{sa} value is calculated to be 12.3 Å. As we know, the resonant energy-transfermechanismconsists of two types: one is exchange interaction and another is multipolar interaction. It is known that if energy transfer takes the exchange interaction, the critical distance between the sensitizer and activator should be shorter than 3-4 Å. Here, the critical distance is longer than 3-4 Å, which indicates the more possibility of energy transfer via the multipolar interaction mechanism.

According to Dexter's energy transfer expressions of multipolar interaction, the following relation can be easily obtained:[25,26]

$$\frac{I_{so}}{I_s} \propto C^{\alpha/3}$$

where I_{so} and I_s are the luminescence intensities of the Ce^{3+} ions with and without the Mn^{2+} ions, and C is the sum of Ce^{3+} and Mn^{2+} concentration. α = 6, 8, and 10 are dipole-dipole, dipole-quadrupole, and quadrupole-quadrupole interaction, respectively. **Fig.9** has shown the plots of I_{so} / I_s of Ce^{3+} vs α = 6, 8, 10. A line relation is well-fit at α = 8, indicating the energy transfer mechanism via a dipole–quadrupole interaction from the Ce^{3+} to Mn^{2+} ions. Considering the dipole–quadrupole mechanism, the critical distance of energy transfer from the Ce^{3+} to Mn^{2+} can be calculated by the spectral overlap method. The energy transfer probability P_{sa}(in s^{-1}) from the Ce^{3+} to Mn^{2+} can be written as:

$$P_{sa} = 3.0\times10^{12}\frac{\lambda_s^2 f_q}{R^8 \tau_S}\int\frac{F_s(E)F_a(E)}{E^4}dE$$

where f_q is the oscillator strength of the involved absorption transition of the acceptor, λs (in Å) is the emission position of the sensitizer(in nm), R is the distance between the activator and

acceptor, τ_S is the decay lifetime of the sensitizer (in seconds). E is the emission energy of the Ce^{3+} ion (in eV), and $\int F_s(E)F_a(E)dE/E^4$ represents the spectral overlap between the normalized shapes of the sensitizer emission and the acceptor excitation. The critical distance R_{sa} between the sensitizer and activator is defined as the distance at which the probability of energy transfer equals the probability of radiative emission of the Ce^{3+} ions. Namely, at the critical distance there has the equation $P_{sa}\tau_s = 1$. Then, R_{sa} can be obtained by the following formula:[27,28]

$$R_{sa}^{\ 8} = 3.0\times10^{12}\lambda_s^2 f_q \int \frac{F_s(E)F_a(E)}{E^4}dE$$

On the basisi of the above equation combined with $f_q = 10^{-10}$, the critical distance R_C was calculated to be11.6 Å , which agrees approximately with that obtained by using the concentration-quenching method.

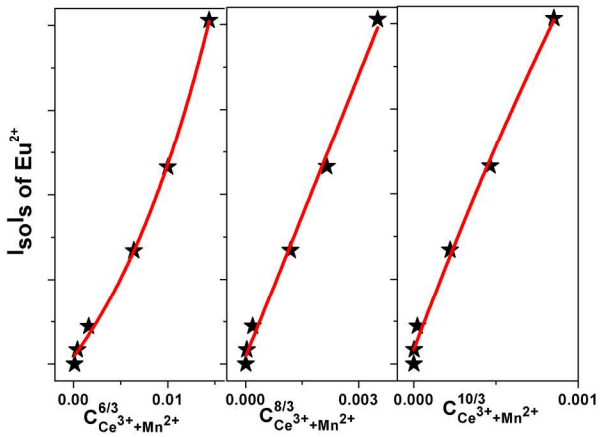

Fig. 9 Dependence of I_0/I of (Ce+Mn) ion concentraction (a) $C^{6/3}$, (b) $C^{8/3}$, and (c) $C^{10/3}$

To determine the quantum efficiency of photoconversion for this phosphor. Herein we applied the integrated sphere method for the measurements of optical absorbance (A) and quantum efficiency (Φ) of the phosphors. The optical absorbance and quantum efficiency of $Na_2Ba_6(Si_2O_7)(SiO_4)_2:Ce^{3+},Mn^{2+}$ phosphors were calculated by using the following two equations:

$$A = \frac{L_0(\lambda) - L_i(\lambda)}{L_0(\lambda)}$$

$$\phi = \frac{E_i(\lambda) - (1-A)\times E_0(\lambda)}{L_e(\lambda)\times A}$$

Where $L_0(\lambda)$ is the integrated excitation profile when the sample is diffusely illuminated by the integrated sphere's surface, $Li(\lambda)$ is the integrated excitation profile when the sample is directly excited by the incident beam, $E_i(\lambda)$ is the integrated luminescence of the sample upon direct excitation, and $E_0(\lambda)$ is the integrated luminescence of the sample excited by indirect illumination from the sphere. The term $Le(\lambda)$ is the integrated excitation profile obtained from the empty integrated sphere (without the sample present). On the basis of the above two equations, the measured values of quantum efficiency were 43.1%, 36.7%, 35.2%, 30.4%, 22.7%, 17.1% in $Na_2Ba_6(Si_2O_7)(SiO_4)_2:0.01Ce^{3+},yMn^{2+}$ phosphor with y = 0, 0.03, 0.07, 0.09, 0.11 material at room temperature under the excitation wavelength of 340 nm. The higher quantum efficiency can be obtained by further improving the synthesis conditions to reduce the number of defects and impurities and to get a high crystallization of the phosphors.

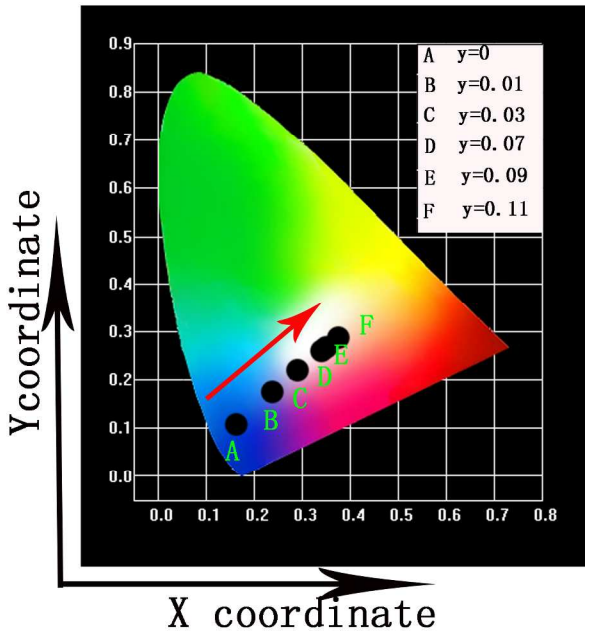

Fig. 10 CIE chromaticity diagram $Na_2Ba_6(Si_2O_7)(SiO_4)_2:0.01Ce^{3+},yMn^{2+}$(0.01, 0.03, 0.07, 0.09, 0.11) phosphors under 340 nm excitation

Fig.10 portrays the CIE chromaticity coordinates for the $Na_2Ba_6(Si_2O_7)(SiO_4)_2:0.01Ce^{3+},yMn^{2+}$(0.01, 0.03, 0.07, 0.09, 0.11) phosphors under 340 nm excitation. Generally, the coordinates shift from blue area (point A) to yellow area (point F) with the increase of Mn^{2+} ion concentration. It is found that the CIE chromatic coordinate is located at (0.348, 0.262) in the white-light area when the concentration of Mn^{2+} ions increases to y = 0.07. And the ideal CIE chromatic coordinate of WLEDs can be got by optimizing the amount of Ce^{3+} ions and Mn^{2+} addition simultaneously. The result indicates the novel $Na_2Ba_6(Si_2O_7)(SiO_4)_2:Ce^{3+},Mn^{2+}$ with tunable color hue has a gteat potential phosphor fo UV-excited WLEDs.

3. Conclusion

In summary, we have synthesized novel $Na_2Ba_6(Si_2O_7)(SiO_4)_2:Ce^{3+}$ and $Na_2Ba_6(Si_2O_7)(SiO_4)_2:Ce^{3+},Mn^{2+}$ phosphors by high temperature solid state method. The $Na_2Ba_6(Si_2O_7)(SiO_4)_2:Ce^{3+}$ phosphor show a broad emission band under UV excitation and excellent thermal stability. The $Na_2Ba_6(Si_2O_7)(SiO_4)_2:Ce^{3+},Mn^{2+}$ phosphor shows tunable color by controlling the composition of Mn^{2+} content. The energy transfer from Ce^{3+}ion to Mn^{2+} ion has been confirmed to be via a dipole–quadrupole mechanism on the basis of the Dexter's energy transfer theory. The involved critical distance of energy transfer has also been calculated by concentration quenching method and spectral overlap method. All the above investigations

show that the novel $Na_2Ba_6(Si_2O_7)(SiO_4)_2:Ce^{3+},Mn^{2+}$ phosphor with tunable emission property has great potential as novel phosphor for UV-WLEDs.

Acknowledgment

This work is financially supported by the National Natural Science Foundation of China (Grant No. 21271167) and the Fund for Creative Research Groups (Grant No. 21221061).

References

1. C. Feldmann, T. Justel, CR. Ronda, P. J. Schmidt, *Adv. Funct. Mater*., 2003, **12**, 511.
2. C.C. Lin, R.S. Liu, *J. Phys. Chem. Lett*., 2011, **2**, 1268–1277.
3. X. Li, J. D. Budai, F. Liu, J. Y. Howe, J. Zhang, X. Wang, Z. Gu, C. Sun, R. S.Meltzer,Z. Pan, *Light Sci. Appl*.,2013,**2**,e50.
4. J. K.Park, M.A. Lim, C. H. Kim, H. D. Park, J. T. Park, S. Y. Choi, *Appl. Phys. Lett*., 2003,**82**, 683.
5. H. S. Jang, D.Y. Jeon, *Appl. Phys. Lett*. 2007,**90**,041906.
6. H. Luo, J. Liu, X. Zheng, L. Han, K. Ren, X. Yu, *J. Mater. Chem*.,2012, **22**, 15887-15893.
7. Z. Tao, Y. Huang, H.J. Seo, *Dalton Trans*. 2013,**42**, 2121-2129.
8. D. Haranath, H. Chander, P. Sharma, S. Singh, *Appl. Phys. Lett*. 2006, **89**, 173118.
9. Y. Q. Li, N. Hirosaki, R. J. Xie, T. Takeda, M. Mitomo, *Chem. Mater.,* 2008**, 20**, 6704–6714.
10. C.Duan, Z. Zhang, S.Rosler, S. Rosler, A. Delsing, J. Zhao, H. T. Hintzen, *Chem. Mater*., 2011, **23**, 1851–1861.
11. W. Lv, W. Lü, N.Guo, Y. Jia, Q. Zhao, M. Jiao, B. Shao, H. You, *Dalton Trans*., 2013, **42,** 13071-13077.
12. T. Armbruster, F. Rothlisberger, *Am. Miner*. 1990,75, 75963–969.
13. A. C. Larson and R. B. Von Dreele, Los Alamos National Laboratory Report LAUR, 1994.
14. C. Liu, H. Liang, X. Kuang, J. Zhong, S. Sun, Y. Tao, *Inorg. Chem*., 2012, **51**, 8802−8809.
15. Y. Jia, H. Qiao, Y. Zheng, N. Guo, H. You, *Phys. Chem. Chem. Phys*., 2012,**14**, 3537-3542.
16. G. Ju, Y. Hu, L. Chen, X. Wang, *J. Appl. Phys*.,2012,111, 113508.
17. L.G.Van Uitert, *J. Lumin*., 1984,**29**,1-9.
18. C. Huang, Y. Chen, T. Chen, T. Chan, H. Sheu, *J. Mater. Chem*., 2011, **21**, 5645.
19. J. Y. Han, W. B. Im, G. Lee, D. Y. Jeon, *J. Mater. Chem*., 2012,**22**, 8793-8798.
20. G. Lee, J. Y. Han, W. B. Im, S. H. Cheong, D. Y. Jeon, *Inorg. Chem*., 2012,**51**, 20.
21. C. Liu, Z. Xia, Z. Lian, J. Zhou, Q. J. Yan, *J. Mater.Chem. C*., 2013, **1**, 7139-7147
22. G.Blass, *J. Chem. Phys*. 1969,**51**, 3529.
23. L. Shi, Y. Huang, H. J. Seo, *J. Phys. Chem. A.,* 2010, **114**, 6927–6934.
24. P.I. Paulose, G. Jose, V. Thomas, N.V. Unnikrishnana, M.K.R. Warrier, *J. Phys. Chem. Solids*., 2003, **64** , 841–846.
25. W. Yang, L. Luo,T. Chen, N. Wang. *Chem. Mater.,* 2005, *17,* 3883-3888.
26. G. Blasse, *Philips Res. Rep*., 1969, **24**, 131.
27. G. Li, D. Geng, M. Shang, Y. Zhang, C. Peng, Z. Cheng, J. Lin, *J. Phys. Chem. C*., 2011, **115**, 21882–21892.
28. H. You, J. Zhang, G. Hong, H. Zhang, *J. Phys. Chem. C*., 2007**, 111**, 10657-10661.